

# Charged basal stacking fault scattering in nitride semiconductors

Aniruddha Konar,<sup>a)</sup> Tian Fang, Nan Sun, and Debdeep Jena

Department of Physics and Department of Electrical Engineering, University of Notre Dame, Notre Dame, Indiana 46556, USA

(Received 24 November 2010; accepted 29 December 2010; published online 14 January 2011)

A theory of charge transport in semiconductors showing built-in polarization (polar) is developed in the presence of basal stacking faults. The theory is based on quantum tunneling in conjunction with the semiclassical description of diffusive charge transport. It is shown that the presence of basal stacking faults leads to anisotropy in carrier transport. The theory is applied to carrier transport in gallium nitride films consisting of a large number basal stacking faults, and the result is compared with experimental data. © 2011 American Institute of Physics. [doi:10.1063/1.3543846]

The III-V nitride semiconductors and related compounds have attracted immense attention for optoelectronic devices<sup>1,2</sup> covering a wide range of the electromagnetic spectrum as well as high-speed, high temperature electronic devices. For *c*-plane grown nitrides, built-in polarization field, although advantageous for two-dimensional (2D) electron gas formation in transistors,<sup>3</sup> reduces the overlap of electron-hole wave function, reducing the oscillator strength for radiative transitions. Moreover, *c*-plane based enhancement mode transistors suffer from low threshold voltages<sup>4</sup> ( $V_{th} \sim 1$  V) impeding their applications in safe circuit operation. A potential way to eliminate these effects is to grow nitrides in nonpolar directions. However, heteroepitaxial, nonpolar, and semipolar nitrides films grown on lattice mismatched substrates contain  $n_{SF} \sim 1 - 10 \times 10^5/\text{cm}$  basal stacking faults (BSFs) parallel to the [0001] direction.<sup>5,6</sup> Directionally dependent transport measurements in highly faulted nonpolar nitride films show strong mobility anisotropy for both electron and hole transport, with mobility parallel to the [0001] direction significantly lower relative to the in-plane [11 $\bar{2}$ 0] mobility.<sup>7-9</sup> This anisotropy has been associated with scattering from BSFs qualitatively, although no quantitative model exists. In this letter, we develop a theory of carrier scattering phenomena from BSFs and a quantitative estimate of the transport anisotropy is presented with comparison to experimental data.

Stacking faults (SF) are 2D structural defects associated with heteroepitaxial growth on lattice-mismatched substrates. Most prevalent SFs in wurtzite (WZ) nitrides is of the  $I_1$ -type requiring lowest energy of formation.<sup>10</sup> Scattering-contrast transmission microscope imaging revealed<sup>5</sup> that the SFs in GaN are primarily of the  $I_1$ -type which corresponds to a stacking sequence of (0001) basal plane  $\cdots ABABABCBCBC \cdots$ . A BSF can be thought as a thin zincblende (ZB) layer (up to three monolayers thick) perfectly inserted in the WZ matrix without broken bonds as shown in Fig. 1(a). The built-in polarization difference between ZB and WZ structures will result in bound sheet charges  $\pm\sigma_\pi$  at each interface of the BSF layer. Consequently, the band edge will bend near the BSF. Figure 1(b) shows a typical conduction band diagram around a BSF for a *n*-doped GaN film along with the charges that are formed in the direction perpendicular to the BSF plane. The bending of

conduction band edge inside the BSF is due the electric field resulting from the polarization bound charge, whereas, bands bend outside the BSF due to the accumulation and depletion of mobile charges. We approximate the accumulation charge as a sheet charge of density  $n_s$  at the centroid ( $t$ ) of the charge distribution, i.e.,  $\rho_\pi(x) = en_s \delta(x - x_0)$ , where  $x_0 = d + t$ ,  $d$  being the width of a BSF and  $e$  is the electron charge. If  $x_d$  is the width of the depletion region, charge neutrality requires  $n_s = x_d N_d$ , where  $N_d$  is the donor density. Energy conservation across the BSF leads to the relation

$$\frac{eN_d x_d^2}{2\epsilon_s} + \frac{en_s t}{2\epsilon_s} = \left( \frac{e\sigma_\pi}{2\epsilon_s} - \frac{en_s}{2\epsilon_s} \right) d, \quad (1)$$

where,  $\epsilon_s$  is the permittivity of the semiconductor. In the limit  $x_d \gg (t, d)$ , the depletion length is  $x_d \approx \sqrt{\sigma_\pi d / N_d}$ . The depletion width  $x_d$  increases with decreasing donor density and there exists a critical donor density  $N_d^{cr}$  for which,  $x_d$  becomes equal to the distance between two SFs. As a result the whole channel is depleted, and conduction ceases along the  $x$  direction. The critical donor density above which onset of conduction along  $x$  direction occurs is given by  $N_d^{cr} \geq \sigma_\pi d n_{SF}$ . For a typical fault density  $n_{SF} = 10^5/\text{cm}$  and  $d = 0.8$  nm for GaN,<sup>11</sup> the critical doping density is  $N_d^{cr} = 10^{16}/\text{cm}^3$ . In the rest of the paper, we will work in the regime where  $N_d \gg N_d^{cr}$ .

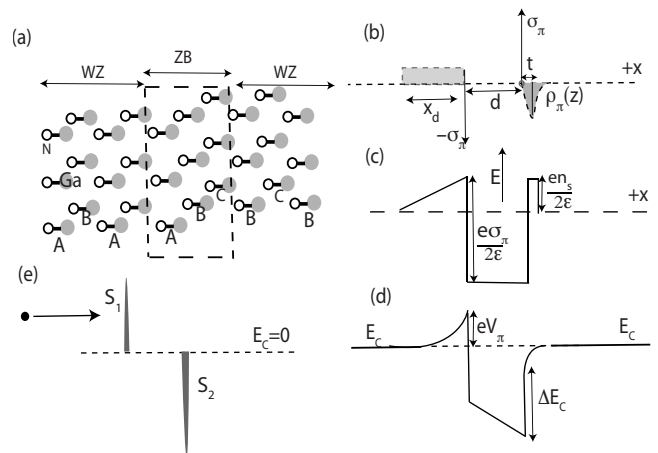


FIG. 1. (a) Structure of BSFs, (b) charges across the BSF, (c) schematic diagram of electric field, (d) conduction band diagram including band offset, and (e) delta function model of barrier and QW.

<sup>a)</sup>Electronic mail: akonar@nd.edu.

In addition to the polarization charges at interfaces, the conduction band offset ( $\Delta E_c$ ) between ZB and WZ structures leads to a quantum well (QW) in the fault region as shown in Fig. 1(b). For an applied bias, electrons tunnel through the barrier (in the depletion region) and QW (in the fault region) and then diffuse in the space between two consecutive SFs. To model the transmission coefficient of tunneling, we approximate the barrier and the QW as two delta functions (as shown in Fig. 1(e) of strengths  $S_1 = eV_\pi x_d$  and  $S_2 = (\Delta E_c + eV_\pi)d$ ; where  $V_\pi = \sigma_\pi d / 2\epsilon_s$ ). The energy dependent coefficient of transmission through a single delta function potential is an analytically solvable problem.<sup>12</sup> If  $T_{tr,1}(\epsilon)$  and  $T_{tr,2}(\epsilon)$  are the transmission coefficient from the barrier and the QW, respectively, then the total coefficient of transmission across the BSF is given by  $T_{tr}(\epsilon) = T_{tr,1}(\epsilon)T_{tr,2}(\epsilon)$

$$T_{tr}(\epsilon) = \left( \frac{1}{1 + \frac{m^* S_1^2}{2\hbar^2 \epsilon}} \right) \times \left( \frac{1}{1 + \frac{m^* S_2^2}{2\hbar^2 \epsilon}} \right), \quad (2)$$

where,  $\epsilon$  is the energy of the incoming electron and  $m^*$  is the effective mass at the band edge. In SF-free structures, the elemental current component along the  $x$  direction for an electron with velocity  $v_k$  is given by  $j_x^k = ev_k^x \delta f_k$ ; where  $\delta f_k$  is the modification of equilibrium Fermi–Dirac distribution caused by an applied electric field  $F_{\text{appl}}$ . In the presence of SFs, a part [given by Eq. (2)] of these carriers is transmitted through the barrier and the QW leading to an effective elemental current density  $j_k^{\text{eff}} = T_{tr}(\epsilon) j_k^x$ . Then, the total current density in the presence of SFs is given by

$$J_x = 2e \int \frac{d^3k}{(2\pi)^3} T_{tr}(\epsilon) v_k^x \delta f_k, \quad (3)$$

where,  $v_k^x$  is the  $x$  component of electron group velocity in the state  $|\mathbf{r}, \mathbf{k}\rangle$  and the factor 2 takes spin degeneracy into account. For a small applied electric field along the  $x$  direction, under the relaxation time approximation,  $\delta f_k \approx (-\partial f_0 / \partial \epsilon) \tau(k) v_k^x F_{\text{appl}}$ , where,  $f_0$  is the equilibrium Fermi–Dirac distribution function and  $\tau(k)$  is the momentum relaxation time due to scattering from impurities, phonons, etc. present in the material. Integrating Eq. (3) over all  $k$ -space and defining conductivity by the relation  $J_x = \sigma(n, T) F_{\text{appl}}$ , one obtains the carrier concentration ( $n$ ) and temperature ( $T$ ) dependent conductivity in the presence of BSFs. The expression for conductivity across the BSF is then given by

$$\sigma_{xx}(T, n) = \frac{3ne^2 \int d\epsilon \epsilon^{1/2} \cosh^{-2}(\epsilon/2k_B T) T_{tr}(\epsilon) \tau(\epsilon) (v_x^k)^2}{8\pi \int d\epsilon \epsilon^{3/2} \cosh^{-2}(\epsilon/2k_B T)}, \quad (4)$$

where  $T$  is the equilibrium temperature and  $k_B$  is Boltzmann constant. Since the BSF does not break the periodic symmetry in the  $y$  and  $z$  directions, inserting  $T_{tr}(\epsilon) = 1$  for all energies, a similar expression can be obtained for conductivity ( $\sigma_{yy}$ ) along the  $y$  direction. For hole transport,  $\Delta E_c$  should be replaced by valence band offset ( $\Delta E_v$ ) in the strength of delta function potential  $S_2$ , and a hole effective mass should be used instead of the electron effective mass.

Equation (4) is the central finding of this work as it allows us to calculate experimentally measurable quantities such as conductivity and mobility in the presence of BSFs. As an application of the formalism constructed above we

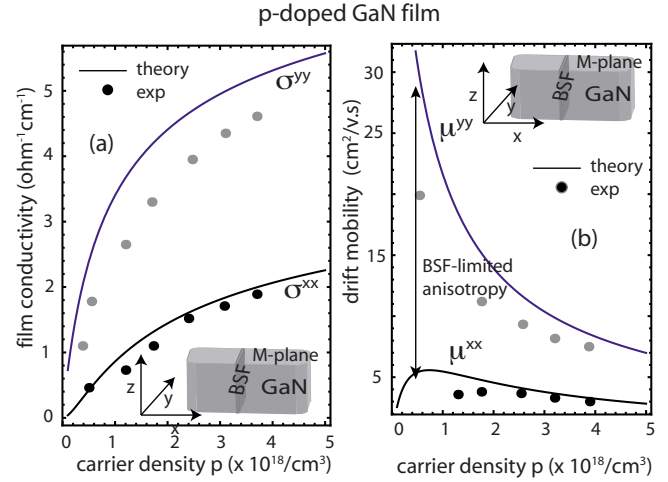


FIG. 2. (Color online) (a) Hole conductivity as a function of hole density: anisotropy is due to BSF. (b) Hole mobility as a function of hole density. Solid lines are theoretical values and solid circles are experimental values from Ref. 7.

investigate charge transport in  $p$ -type  $m$ -plane (1 $\bar{1}$ 00) GaN in the presence of BSFs, and compare the results with previous reported experimental data. Inclusions of different scattering mechanisms are necessary to evaluate the energy dependent momentum relaxation time  $\tau(\epsilon)$  appearing in Eq. (4). Due to the high activation energy of acceptors [Mg for  $p$ -type GaN has activation energy  $\sim 174$  meV (Ref. 7)], a large fraction of the dopants remain neutral even at room temperature, acting as neutral impurity scatterers to hole transport. Accounting for the zero-order phase shift,<sup>13</sup> the momentum relaxation time of neutral impurity scattering is  $\tau_{\text{NI}}^{-1} = 20N\hbar a_0 / m^*$ ; where  $N$  is the density of neutral impurities and  $a_0 = 4\pi\epsilon_s \hbar^2 / m^* e^2$  is the effective Bohr radius. Momentum relaxation time due to ionized impurity scattering ( $\tau_{\text{imp}}$ ) is calculated following the method of Brooks–Herring.<sup>14</sup> For electron-optical phonon momentum-relaxation time ( $\tau_{\text{ph}}$ ), only phonon absorption has been considered due to the high optical phonon energy ( $E_{\text{op}} = 0.092$  eV  $\gg k_B T$ ) of GaN. The resultant momentum-relaxation time is calculated using Mathiessen's rule; i.e.,  $\tau(\epsilon)^{-1} = \tau_{\text{NI}}^{-1} + \tau_{\text{imp}}^{-1} + \tau_{\text{ph}}^{-1}$ . For numerical calculations, we assume the valence band offset  $\Delta E_v = 0.06$  eV.<sup>10</sup> The hole effective mass of GaN is not well known and a wide range  $m_h^* = 0.4 - 2.4m_0$  ( $m_0$  is the rest mass of a bare electron) is found in existing literature.<sup>2</sup> In this work, we have assumed  $m_h^* \sim 1.8m_0$ . Neutral impurity density is chosen to be  $N = 24 \times p$ , where  $p$  is free hole concentration in GaN. This choice is not *ad hoc*; measurements<sup>7</sup> show that the neutral impurity density  $N = N_A - p \approx 20 - 25 \times p$  for a wide range of acceptor densities  $N_A$ . This high density of neutral impurities makes neutral impurity scattering dominant over other scattering mechanisms at room temperature.

Figure 2(a) shows the calculated (solid lines) variation of  $\sigma_{xx}$  (along the  $c$ -axis) and  $\sigma_{yy}$  (parallel to  $a$  axis) as a function of hole density at room temperature juxtaposed with experimental<sup>7</sup> data (filled circles). It is apparent from the figure that the presence of BSF causes an appreciable reduction of  $\sigma_{xx}$  compared to  $\sigma_{yy}$ , resulting in anisotropic hole transport. The corresponding hole mobility  $\mu_{ii} = \sigma_{ii} / pe$ ;  $i = x, y$ , is shown in Fig. 2(b). The anisotropy in hole mobility increases with decreasing hole density. This stems out from

the fact that, in the limit  $p \rightarrow 0$ , the depletion width increases ( $x_d \sim N_A^{-1/2}$ ) and one approaches the critical acceptor density limit  $N_A^{cr}$ . As  $x_d$  increases, the strength of the barrier  $S_1$  increases, and  $T_{tr}(\epsilon) \rightarrow 0$ . This results in vanishing  $\mu_{xx}$  ( $\sigma_{xx}$ ; see Fig. 2).

An important observation is that the anisotropy in hole mobility decreases with increasing carrier concentration. At higher carrier densities, transmission of carriers occupying higher energy states approaches unity ( $T_{tr}(\epsilon) \rightarrow 1$ ) leading to  $\mu_{xx} \sim \mu_{yy}$ . The corresponding carrier density is  $p_0 \approx 1/3 \pi^2 (m^* \Delta E_v d / \hbar^2)^3 (\sim 10^{19} / \text{cm}^3)$ , above which BSF-induced transport anisotropy vanishes in nonpolar GaN. At high acceptor concentrations, the energy levels of impurity atoms overlaps to form impurity bands. While conduction through this impurity band is important at low temperatures, at room temperature impurity band does not form an efficient transport path<sup>15</sup> and its exclusion from our model is quite justified. Our work presented here can be improved in three ways: (i) at low carrier densities  $x_d$  is large; assumption of the delta function barrier breaks down and one should solve the Schrodinger equation numerically to obtain exact transmission coefficient  $T_{tr1}(\epsilon)$ , and (ii) at low doping levels (when  $x_d$  is large) or for high SF density, carriers are confined in a quasi-two dimensional space rather than moving in three dimensions. Hence, one should use a 2D analog of Eq. (4) for an exact evaluation of  $\mu_{yy}$ , and (iii) by incorporating the contributions of quasilocalized<sup>11</sup> electrons in the shallow state of the thin QW located in the fault region.

High-quality (low defect densities) nonpolar GaN is currently under development. It is apparent that with decreasing SF density, transport anisotropy will decrease and eventually vanishes for BSF free nonpolar GaN films. The theory presented here is not only applicable to GaN, but to any semiconductor [including other members of the nitride family such as InN and AlN (Ref. 6)] having BSFs with proper choice of material parameters. For example, the semiconductor zinc-oxide shows SFs similar to GaN with  $\sigma_\pi = 0.057 \text{ C/m}^2$  and the band offsets<sup>16</sup> are  $\Delta E_c = 0.147 \text{ eV}$  and  $\Delta E_v = 0.037 \text{ eV}$ .

In summary, we have presented a transport theory in semiconductors containing a large number of BSFs. The theory is applied to understand the experimentally observed transport anisotropy in  $m$ -plane GaN and a reasonable agreement between theory and experiment is obtained. Two critical limits of carrier concentration are derived, one where transport across a BSF ceases and another, where the presence of BSFs can be ignored in the context of charge transport.

The authors would like to acknowledge J. Verma and S. Ganguly (University of Notre Dame) for helpful discussions and National Science Foundation (NSF) (NSF Grant Nos. DMR-0907583 and NSF DMR-0645698), Midwest Institute for Nanoelectronics Discovery (MIND) for the financial support for this work.

<sup>1</sup>P. Waltereit, O. Brandt, A. Trampert, H. T. Grahn, J. Menniger, M. Ramsteiner, M. Reiche, and K. H. Ploog, *Nature (London)* **406**, 865 (2000).

<sup>2</sup>J. Piprek, *Nitride Semiconductor Devices: Principles and Simulations* (Wiley, Weinheim, 2007).

<sup>3</sup>C. Wood and D. Jena, *Polarization Effects in Semiconductors: From Ab Initio Theory to Device Applications* (Springer, New York, 2008).

<sup>4</sup>Y. Cai, Y. Zhou, and K. J. Chen, *IEEE Electron Device Lett.* **26**, 435 (2005).

<sup>5</sup>B. A. Haskell, A. Chakraborty, F. Yu, H. Sasano, P. T. Fini, S. P. DenBaars, J. Speck, and S. Nakamura, *J. Electron. Mater.* **34**, 357 (2005).

<sup>6</sup>K. Ueno, A. Kobayashi, J. Ohta, and H. Fujioka, *Jpn. J. Appl. Phys.* **49**, 060213 (2010).

<sup>7</sup>M. McLaurin, T. E. Mates, F. Wu, and J. S. Speck, *J. Appl. Phys.* **100**, 063707 (2006).

<sup>8</sup>M. McLaurin, T. E. Mates, and J. S. Speck, *Phys. Status Solidi (RRL)* **1**, 110 (2007).

<sup>9</sup>K. H. Baik, Y. G. Seo, S. Hong, S. Lee, J. Kim, J. Son, and S. Hwang, *IEEE Photonics Technol. Lett.* **22**, 595 (2010).

<sup>10</sup>C. Stampfl and C. G. Van de Walle, *Phys. Rev. B* **57**, R15052 (1998).

<sup>11</sup>Y. T. Rebane, Y. G. Shreter, and M. Albrecht, *Phys. Status Solidi A* **164**, 141 (1997).

<sup>12</sup>D. J. Griffiths, *Introduction to Quantum Mechanics* (Pearson Education, Singapore, 2005).

<sup>13</sup>C. Erginsoy, *Phys. Rev.* **79**, 1013 (1950).

<sup>14</sup>H. Brooks, *Phys. Rev.* **83**, 879 (1951); D. Chattopadhyay, and J. J. Queisser *Rev. Mod. Phys.* **53**, 745 (1981).

<sup>15</sup>D. Lancefield and H. Eshghi, *J. Phys.: Condens. Matter* **13**, 8939 (2001).

<sup>16</sup>Y. Yan, G. M. Dalpian, M. M. Al-Jassim, and S. Wei, *Phys. Rev. B* **70**, 193206 (2004).